Reprinted from AIChE JOURNAL, March 1976

Mathematical Models of the Monolith Catalytic Converter:

Part II. Application to Automobile Exhaust

Calculations are done for a series of mathematical models for a monolith catalytic converter to oxidize carbon monoxide in automobile exhaust. Phenomena studied include axial conduction in the wall, diffusion and conduction in the gas in a transverse direction perpendicular to the flow direction, multiple steady states, and transients giving wall temperatures exceeding the adiabatic temperature.

LARRY C. YOUNG

and

BRUCE A. FINLAYSON

Department of Chemical Engineering
University of Washington
Seattle, Washington 98195

SCOPE

For better or for worse, the use of catalytic converters to reduce automobile emissions of carbon monoxide and hydrocarbons has become a reality. Two types of catalytic converters are used for this application: packed beds and monoliths. The present study is concerned with mathematical models for the monolith converter. The simplest model which will give realistic predictions is determined, and the model calculations illustrate the important phenomena occurring in the device.

Although considerable attention has been devoted to modeling packed-bed converters (Wei, 1975), little published information is available on modeling monolith converters. Kuo (1973) developed a lumped parameter model for the monolith converter, which has been used by eight automobile and oil companies. Votruba et al. (1975) have also presented a similar model. Both these models include axial conduction in the wall. Hegedus (1974) neglects axial conduction. In a preliminary study, Young and Finlayson (1974) proposed and solved two models for the monolith, which cast some doubt on the validity of the simpler models. The essential question is whether or not to include diffusion and conduction in the fluid in a transverse direction perpendicular to the flow (and duct) axis, as did Young and Finlayson, or whether a simple lumped parameter model of this phenomenon, with specified Nusselt and Sherwood numbers,

Larry C. Young is with Amoco Production Company, Tulsa, Oklahoma.

is sufficient, as was done by Kuo, by Hegedus, and by Votruba et al.

In the present study, calculations are done for a series of mathematical models. Comparison of the results enables the choice of the simplest model which can be used for realistic predictions. The question of diffusion and conduction perpendicular to the flow axis is considered, as well as the importance of axial conduction in the wall and peripheral diffusion and conduction in the wall around the duct. The effect on the reaction rate of diffusion limitations in the porous substrate is also included. The results provide a complete study of the types of phenomena occurring in monolith devices.

One of the important limitations to the use of monolith reactors in automobiles is peak overtemperatures which cause the solid walls to melt or deform, which eventually leads to the destruction of the device (Morgan, et al., 1973). Calculations are done to investigate this phenomenon and its dependence on transverse diffusion and conduction in the fluid, axial conduction, and the presence of significant amounts of hydrogen. Model calculations also illustrate the effect of different duct shapes on the performance of the converter. Steady state and transient simulations are included, with transient models being especially important for application to automobile exhaust.

CONCLUSIONS AND SIGNIFICANCE

The most important transport phenomenon which must be included in a model of the monolith reactor is the diffusion and conduction of species and energy in the fluid in a transverse direction perpendicular to the duct axis. Lumped parameter models with Nusselt and Sherwood numbers assigned a priori do not suffice unless multiple steady states are not predicted. Unfortunately, for realistic conditions for treatment of automobile exhaust, multiple steady states are predicted to occur, and lumped parameter models are unsuitable.

Axial conduction in the solid is sometimes important, and its inclusion in the model tends to reduce the temperature gradient at the point where the reaction lights off and to reduce the peak overtemperature during transient and steady state simulations. Both effects tend to shorten the computation time for transient simulations when axial conduction is included rather than excluded. Peripheral variations of temperature and concentration around the duct at a given axial location are predicted to occur, but the effect on the overall performance of the converter is negligible. If hydrogen is modeled as a separate species, rather than relating it strictly to the carbon monoxide concentration, the peak overtemperatures are larger, but still not sufficient to cause melting of the converter during normal operation of the automobile.

MODEL DEVELOPMENT

The monolith converter consists of a number of cells or ducts through which the exhaust gas flows. A diagram of a single square cell is shown in Figure 1. Other cell shapes are possible, and those considered in this study are shown in Figure 2.

The monolith converter consists of the three regions shown in Figure 1: a laminar flow region, a porous catalytic layer, and a relatively nonporous substrate. A cell is typically 1.3 mm wide, the catalytic layer is approximately 0.025 mm thick, and the substrate is typically 0.25 mm thick. A typical converter will contain thousands of these cells. After an initial length in which the velocity profile develops, the fluid flows in laminar flow through each cell. The reactants in the fluid diffuse to the wall and into the catalytic layer, where the reaction occurs; the heat generated and the reaction products diffuse back to the fluid and are carried downstream. All of the models studied here embody the assumption that the velocity profile of the fluid is fully developed

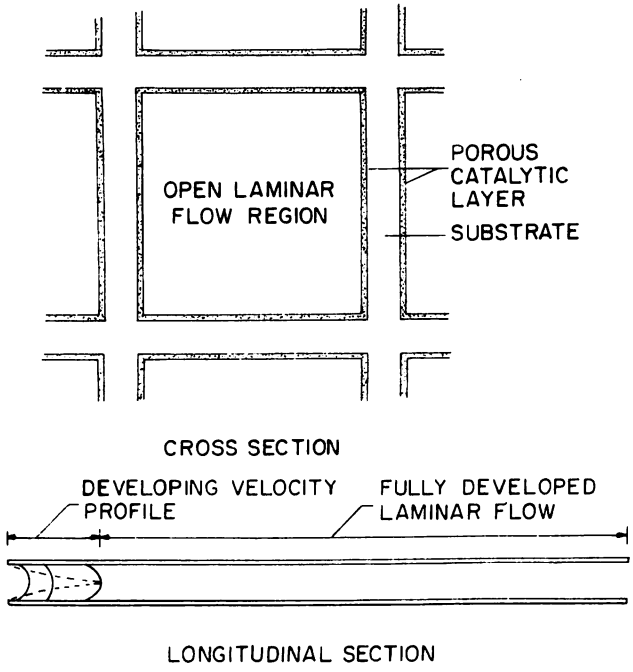

Fig. 1. Cross section and longitudinal section of the square cell.

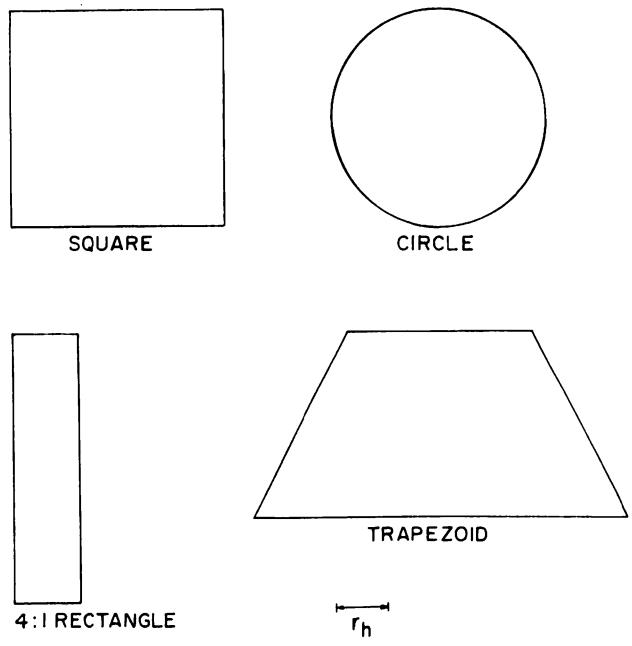

Fig. 2. Cross sections used in this study. Compared at constant r_h.

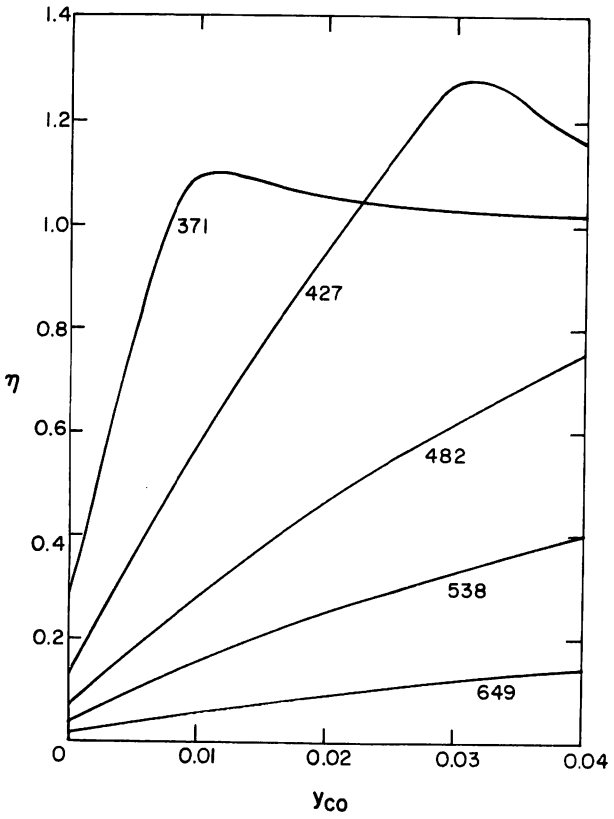

Fig. 3. Effectiveness factors for rate expression P2. D^f_{CO}/D^s_{CO} = 70. Temperatures shown in °C.

TABLE 1. RATE EXPRESSIONS

$$P1: -r_{CO} = \frac{5\,340\ y_{O_2} y_{CO}}{y_{O_2} + 1.33\ y_{CO}^2 \exp(6\,111\ °K/T)} \frac{\text{kg mole}}{\text{sm}^3}$$

$$P2: -r_{CO} \frac{\left(\frac{4.67 \times 10^{16}}{T}\right) y_{O_2} y_{CO}\ e^{-12\,256°K/T}}{(1 + 65.5\ e^{961°K/T}\ y_{CO})^2} \frac{\text{kg mole °K}}{\text{sm}^3}$$

throughout the converter, since a detailed analysis reveals that the effect of the velocity profile developing near the inlet is small. The models embody the assumption that heat conduction perpendicular through the wall is sufficiently fast that temperature variations in this direction are small. The interaction of diffusion and reaction in the catalytic layer in the direction perpendicular to the wall is accounted for by either using an apparent reaction rate based on the conditions at the fluid-solid interface or by using a conventional effectiveness factor. The validity of these assumptions are considered in detail elsewhere (Young, 1974), and they appear to be valid provided that diffusion and reaction in the catalytic layer do not interact to cause multiple steady state solutions. This latter result does not appear likely for parameter values of interest.

The model equations are developed from the fundamental equations of change in Part I. The different models and the phenomena they include are summarized in Table 4 of Part I, to which the readers should refer frequently to orient their thinking. The only part of the model not discussed in detail in Part I is the reaction kinetics, which is discussed below.

Typically, a platinum catalyst is used in the monolith converter. The oxidation of carbon monoxide on platinum is generally agreed to be first order in oxygen and inversely proportional to carbon monoxide (Langmuir,

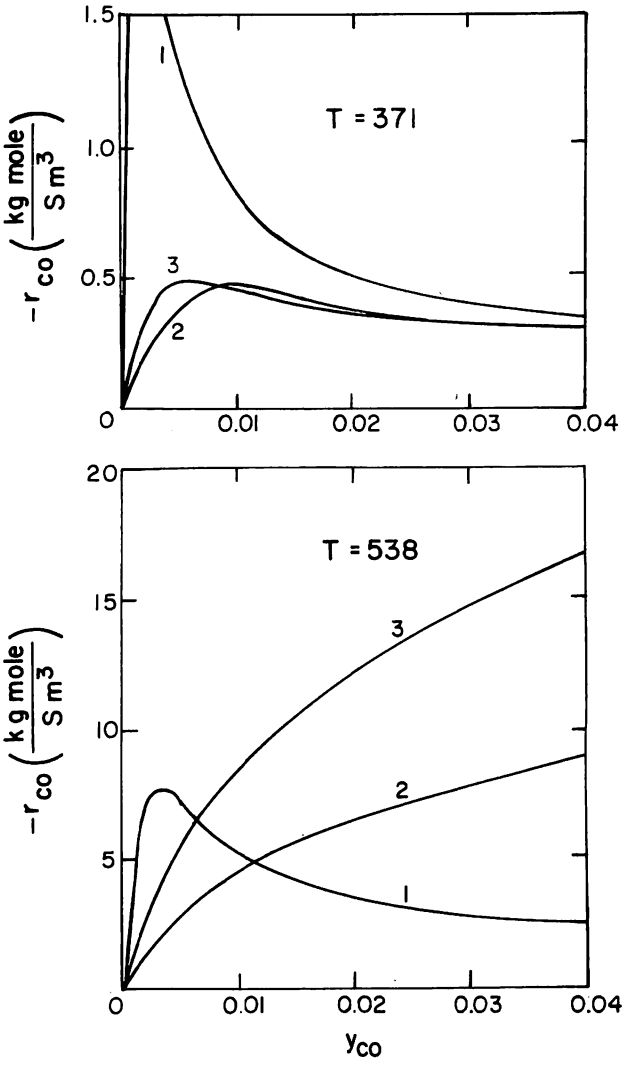

Fig. 4. Apparent rate of reaction (including diffusional limitations). 1—Kinetics P1; 2—Kinetics P2, D^f_{CO}/D^s_{CO} = 70; 3—Kinetics P2, D^f_{CO}/D^s_{CO} = 20.

1922; Harned, 1972; Schlatter et al., 1973; Wei, 1975). The rate expression is negative order in carbon monoxide owing to the strong adsorption of carbon monoxide on platinum. Exact kinetic information is not available. We use here the expression P1 in Table 1 which approximates the data reported by Sklyarov et al. (1969) for the oxidation of carbon monoxide on platinum wire, as well as the data for reaction in porous catalysts by Harned (1972). Expression P1 is assumed to be an apparent reaction rate and embodies internal diffusion effects. The second rate expression, (P2 in Table 1) used is that determined by Voltz et al. (1973). It was determined from data taken only at low temperature ($T < 400°C$) so that the effects of diffusion in the catalyst would be small. Expression P2 is then regarded as an intrinsic reaction rate expression.

The equation for diffusion and reaction in the catalyst, Equation (52) of Part I, is solved by using a combination first-order collocation-asymptotic expansion (Finlayson, 1974). By using reaction kinetics P2 in Table 1, the maximum error in the apparent reaction rate is only 3% over the entire concentration and temperature range of interest. The effectiveness factors calculated in this manner are shown for $D^f_{CO}/D^s_{CO} = 70$ in Figure 3. The resulting apparent reaction rate for P2 is compared to P1, which is assumed to be an apparent rate, in Figure 4.

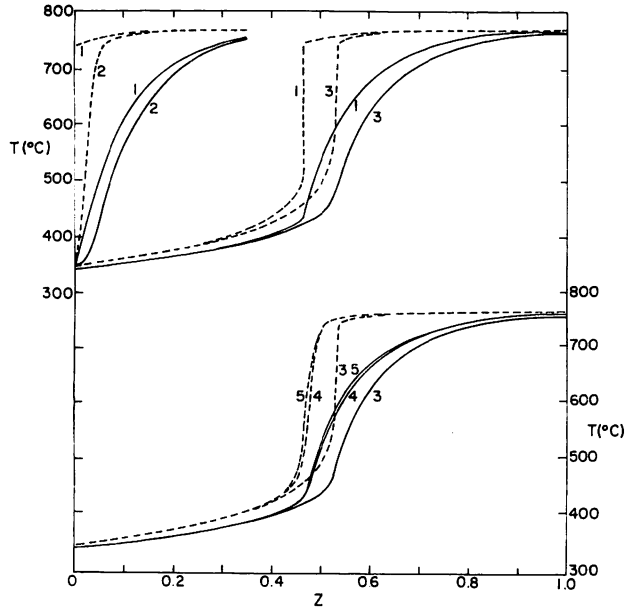

Fig. 5. Steady state model predictions. Inlet T = 344°C and y_{CO} = 4%. $\hat{G}$ = 0.0132 m³/s ----- Solid temperature, ——— Fluid average temperature; 1—Model I, 2—Model I-A, $Nu = Sh = 3.5$; 3—Model II, 4—Model II-A, 5—Model III-A. Square duct $P1$ kinetics.

Interestingly, at high temperature, internal diffusion changes the negative order carbon monoxide dependence of the apparent rate.

In the model calculations, several assumptions regarding the hydrogen and hydrocarbon reactions are made. As assumed by Kuo et al. (1971), the ratio of hydrogen to carbon monoxide is assumed to be 1:3 everywhere in the converter, and the heat of reaction is determined accordingly. The concentration of oxygen in the reactor is assumed to be determined by stoichiometry; that is

$$y^f_{O_2} = y^f_{O_2,o} - 1/2(y^f_{CO,o} - y^f_{CO}) - 1/2(y^f_{H_2,o} - y^f_{H_2})$$

$$y^f_{O_2} = \frac{2}{3}(E + y^f_{CO})$$

and $E = 0.03$ in the calculations. These assumptions are strictly valid only when the ratio of hydrogen to carbon monoxide is 1:3 at the reactor inlet, when the reaction rate of hydrogen is one third of that for carbon monoxide, and when the diffusivities of hydrogen, carbon monoxide, and oxygen are all equal. Since oxygen is usually present in considerable excess, this assumption regarding its concentration should give satisfactory results. Langmuir (1922) reports that hydrogen reacts in a manner similar to carbon monoxide on a platinum catalyst, and the inlet ratio of hydrogen to carbon monoxide is usually assumed to be determined by the equilibrium of the water-gas shift reaction, which gives an inlet ratio of roughly 1:3. [Wei (1975) lists ratios from 1:2 to 1:4.] On the other hand, the diffusivity of hydrogen is much greater than that for carbon monoxide. Some of the calculations below are made by modeling hydrogen as a separate specie to test the importance of this last assumption.

Hydrocarbons are present in very low concentrations and do not contribute a great deal to the heat generated in the converter. Even though Harned (1972) and Voltz et al. (1973) report coupling between the hydrocarbon and carbon monoxide reactions and the outlet concentration of hydrocarbons is important, they are not included in the calculations. The present study is aimed at determining the essential features of the converter which must be included in a converter model.

TABLE 2. CONVERTER GEOMETRIC PROPERTIES

r_h = 0.305 mm
ϵ = 2/3
L = 0.102 m
A_c = 5.53×10^{-3} m²
ζ = 0.0152 mm for $P1$; 0.0254 mm for $P2$
e_s = 0.4

In all, five converter models listed in Table 4 of Part I have been solved numerically by using the orthogonal collocation method as described in Part I. Unless otherwise specified, the geometric properties of the converter are specified at the values shown in Table 2. Physical property values and other constants are listed in the nomenclature of Part I. These parameter values correspond closely to those of an Engelhard PTX-4 converter.

The parameters in Table 2 specify everything about the converter geometry except the cell shape; shapes considered here are shown in Figure 2. The shapes are compared for constant hydraulic radius, void fraction, superficial surface area, converter frontal area, and converter length, that is, those parameters listed in Table 2. Although the pressure drop through monoliths is usually small, the pressure drops will not be the same when this comparison is used. The pressure drop will decrease as follows: rectangle, circle, square, and trapezoid.

MODEL DISCRIMINATION

The converter models have been compared for a number of inlet conditions, flow rates, and rate expressions (including first order). A typical comparison of all five models is shown with $P1$ kinetics used in Figure 5.

The comparison of models I and II was the subject of a previous paper (Young and Finlayson, 1974) and illustrates the importance of transverse diffusion and conduction compared to a lumped parameter model. The equations for model I are the same as those studied by Liu and Amundson (1962) and exhibit multiple solutions for some rate expressions and parameter values. The analysis of Liu and Amundson can be applied directly to determine the conditions under which multiple solutions can occur for the parameter values in Table 2 and the rate expressions in Table 1. With both rate expressions $P1$ and $P2$, model I predicts multiple solutions over a wide range of conditions, and this range is increased by small values of the Nusselt and Sherwood numbers. In Figure 5 the highest and lowest temperature solutions for model I are shown. The lowest solution is typical of a situation where the converter is heated from an initial low temperature, while the highest solution results when the converter is cooled from some initial high temperature. An infinite number of steady state solutions are possible, and they lie between those shown in Figure 5.

Interestingly enough, model II can predict but one steady state solution, provided that diffusion and reaction in the catalytic layer do not interact to cause multiple solutions to Equation (52) of Part I (Young, 1974). Figures 3 and 4 illustrate that this last possibility does not occur for parameters of interest, even though the form of the rate expression might allow it. Figure 5 shows that the lowest solution to model I predicts a discontinuous axial solid temperature profile. A discontinuous profile will always cause the distributed parameter fluid model II to predict infinite Nusselt and Sherwood numbers, and model I with infinite Nusselt and

TABLE 3. VALIDITY OF DIFFERENT MODELS

Steady state conditions	Valid models	Invalid models
1. When reaction rate and transport rates allow multiple steady states [determine using Liu and Amundson (1962) analysis]:		
a. High inlet temperature and concentration; model II-A predicts either complete conversion or a reduction zone at the inlet	All models	None
b. Intermediate inlet temperature; model II does not predict complete conversion, but does predict light off	I (lowest T solution) II, II-A, III-A	I (highest T solution) I-A
c. Low inlet temperature and concentration; model II-A may predict two solutions, one of which doesn't light off (as in Figure 8)	II-A	I, I-A, II
d. Lowest inlet temperature and concentration; model II-A does not light off	I, I-A (lowest T solution) II, II-A, III-A	I, I-A (highest T solution)
2. When reaction rate and transport rates preclude multiple steady states	All	None
Transient conditions		
1. Heating (T^s everywhere increasing)	All models	None
2. Cooling (T^s anywhere decreasing) as in deceleration (Figure 9)	II-A, III-A	I, I-A (may approach wrong steady state) I, I-A II (peak T^s too high)

Phenomena	Model:	III-A, II-A	II	I-A	I
Number of steady state solutions		1 or 2	1	1 or 2	∞
Peak transient wall temperature		Intermediate	Highest	usually none	
Peak temperature due to hydrogen		Lower	High	High	Highest

Sherwood numbers can predict but one steady state solution. Model II does not predict infinite Nusselt and Sherwood numbers in the reaction zone, since there is no discontinuity; however, Figure 6 shows that the Nusselt and Sherwood numbers predicted by model II do reach large values in the reaction zone. In model II, as the reaction lights off, the heat transfer coefficient automatically increases, thus negating the possibility of multiple steady states occurring.

Both models I and II neglect axial conduction and diffusion in the solid phase. Eigenberger (1972) has made computations with a packed-bed reactor model which is essentially the same as model I-A and compares these results to those predicted by model I for conditions under which model I predicts multiple solutions. He finds that the two models can predict vastly different results. For this reason, the importance of using a distributed parameter fluid model is also discussed by comparing models I-A and II-A. The reader should recall that both of these models include the axial conduction and diffusion effects and they only differ by the fluid model used. The validity of model I-A is important also, since this model is essentially the same as that developed by Kuo (1973) and Votruba et al. (1975), which is currently being used by industry.

Typical predictions of models I-A and II-A are illustrated as curves 2 and 4 in Figure 5. Both of these models can, in principle, predict multiple steady state solutions, but, for the conditions illustrated, only a single solution exists. It is apparent from the results shown in the figure and from the results of Eigenberger (1972) that the prediction of model I-A will usually be erroneous. Transverse diffusion and conduction in the fluid are important, and a lumped parameter model is not sufficient, whether or not axial conduction is included.

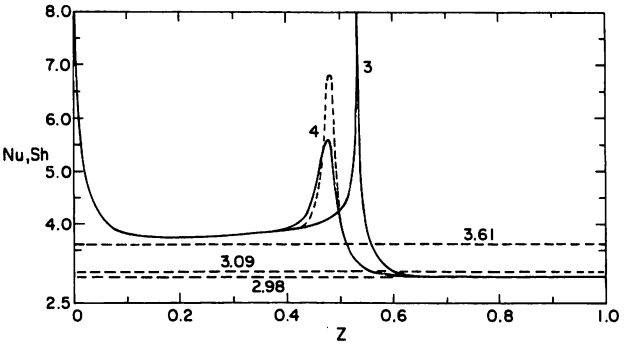

Fig. 6. Nusselt and Sherwood numbers. Inlet conditions as in Figure 5. ——— *Nu*, - - - - *Sh*; 3—Model II, 4—Model II-A.

Figure 5 shows that the lowest solution to model I agrees most closely with model II. Also, the solutions to models II-A and III-A (adding in axial and peripheral conduction) are in fair agreement with those of model II. Thus, the lowest solution to model I and the solutions to models II, II-A, and III-A are usually roughly in agreement. On the other hand, Eigenberger (1972) finds that when the lowest solution to model I corresponds to a reaction that lights off at some point in the converter, when axial conduction is added in model I-A, there is only a single solution, and it corresponds closely to the highest solution of model I. Thus, the lowest solution to model I and the solutions to models II, II-A, and III-A usually agree roughly, and the highest solution to model I and the solution of model I-A agree. Since the highest solution to model I is erroneous, the solution to model I-A is also erroneous.

We can now state limits on the validity of models I and I-A and summarize them in Table 3. If the reaction

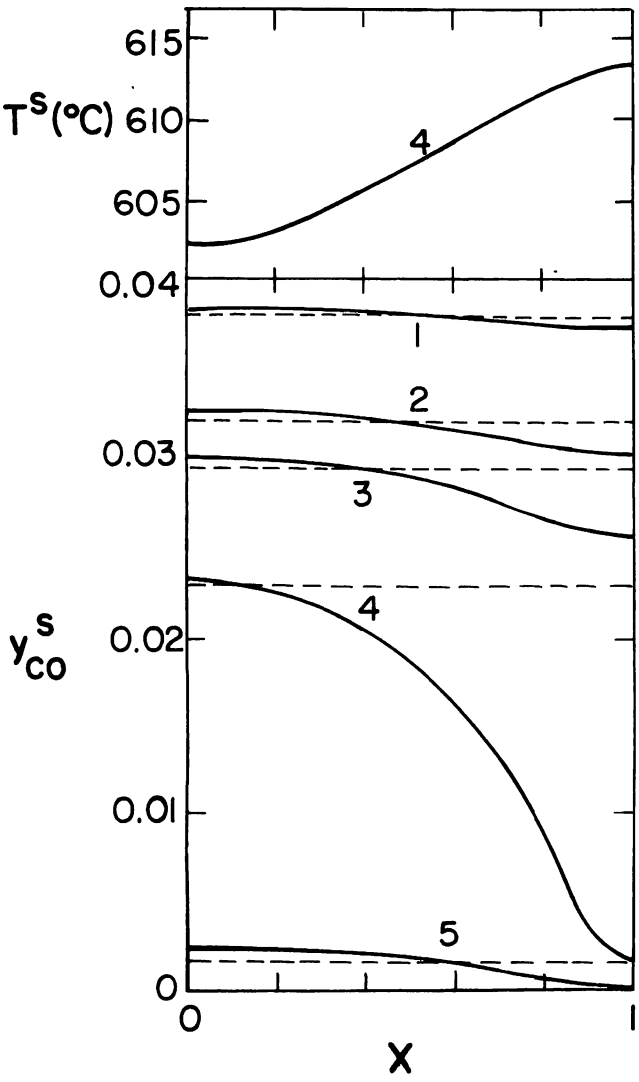

Fig. 7. Peripheral variations of wall temperature and concentration for square. $X = 1$ corresponds to the corner, and $X = 0$ is halfway between corners. Inlet conditions as in Figure 5. ——— Model III-A, - - - - - Model II-A. Axial locations at z = 1—0.1, 2—0.4, 3—0.45, 4—0.475, 5—0.5.

kinetics are such that model I predicts only a single steady state solution, then both models I and I-A will be adequate. The number of steady states predicted by model I can be determined by applying the simple procedures outlined by Liu and Amundson (1962). For the reaction kinetics which occur in practice, model I predicts multiple solutions over a wide range of conditions. In this case only the lowest solution to model I resembles those predicted by the more comprehensive models, and the solution to model I-A and the highest solution to model I will be erroneous. This result justifies the entries in Table 3 under steady state 1b.

These conclusions as to the validity of model I-A are in contrast to current industrial practice. Model I-A was proposed by Kuo (1973) and Votruba et al. (1975) and has been used extensively by industry. There is one possible exception to our conclusions. If the solid thermal conductivity and/or wall thickness are much greater than the typical values used here, then model I-A may become valid. This speculation is advanced because, as shown in Figure 6, axial conduction decreases the magnitude of the Nusselt and Sherwood numbers in the reaction zone. In the limit of large thermal conductivity, the peak values of the Nusselt and Sherwood numbers might be reduced to the final asymptotic values so that models I-A and II-A would agree. These conditions are far removed from those that occur in practice, however.

The Nusselt and Sherwood numbers for the *P*1 kinetics with models II and II-A are shown in Figure 6. Unlike the circular duct, there are three fundamental asymptotic Nusselt numbers for square and other two-dimensional ducts. In addition to the constant temperature problem there are two constant flux problems. The first is constant flux axially and peripherally, and the second is an axially constant peripherally averaged flux with constant temperature around the periphery. For the square duct, the asymptotic Nusselt numbers are 2.98, 3.09, and 3.61, respectively. These asymptotic values are illustrated on the figures for comparison. For model II, the Nusselt and Sherwood numbers are equal. From Figure 6 it is apparent that axial conduction reduces the peak values of the Nusselt and Sherwood numbers in the reaction zone. This result occurs because axial conduction reduces the magnitude of the axial gradients in the solid. Since axial diffusion is unimportant, the peak value of the Sherwood number in the reaction zone is greater than the peak value of the Nusselt number.

By observing the Nusselt and Sherwood numbers in Figure 6, the monolith can be characterized as follows. In the reaction limited region, the Nusselt and Sherwood numbers from the solution of models II and II-A and the Nusselt number from model III-A approach the asymptotic values for constant average flux and uniform temperature around the periphery, 3.61 for the square. In this region, the Sherwood number from model III-A (not shown in Figure 6) approaches the asymptotic value for axially and peripherally constant flux, 3.09 for the square. When the reaction lights off, the Nusselt and Sherwood numbers rise drastically and then decrease to the constant temperature value (2.98) in the mass transfer limited region.

By comparing the results for models II and II-A, curves 3 and 4 in Figure 5, it is apparent that axial conduction and diffusion shifts the reaction zone upstream. The distance the reaction zone is shifted is greater when the axial temperature gradients in the solid are large. As discussed below, with *P*2 kinetics the effect is more severe than that illustrated in Figure 5. Calculations have also been performed with finite axial conduction with no axial diffusion. The results of these calculations agree closely with those of model II-A, so it can be concluded that the difference in the predictions of models II and II-A is due exclusively to axial conduction.

By comparing the predictions of models II-A and III-A, curves 4 and 5 in Figure 5, the effect of finite rather than infinite peripheral conduction and diffusion can be determined. From these figures it is apparent that when peripheral variations are included in a model, the reaction zone is shifted only slightly.

The small discrepancy between the predictions of models II-A and III-A appears to result primarily because of slow diffusion around the periphery. The variation of mole fraction and the maximum temperature variation around the periphery are compared for models II-A and III-A in Figure 7. For this case, the maximum temperature variation is on the order of 12°C. In other cases, the peripheral temperature variations are also small. Calculations have also been performed with zero instead of finite peripheral diffusion, and the results are essentially the same as those shown in Figure 7. Thus, peripheral diffusion is negligible. The fact that model II-A assumes no variations around the periphery and

gives good predictions illustrates that the reaction is much less sensitive to mole fraction than to temperature.

The discrepancy between the solution of models II and II-A, including axial conduction, is sometimes greater than that shown in Figure 5. Hlaváček and Votruba (1974) have experimentally demonstrated that multiple steady states can occur in monolith converters. Although their converter was substantially different from those used in automotive application, it is of interest to see if the models can predict this phenomenon.

Model I usually predicts an infinite number of steady states and is then invalid. Eigenberger (1972) has illustrated that model I-A can have two or three steady states depending on the axial boundary conditions. For the boundary conditions used here, only two steady states result with model I-A; however, model I-A is not always valid either. It can be proven theoretically that model II can have only one steady state, so the important question is, can models II-A or III-A predict multiple steady states?

A case in which model II-A predicts two steady states is shown in Figure 8. In this case, model II would predict light off with a reaction zone at the outlet if the flow rate were reduced to 0.0159 m³/s. Since model II does not predict light off, there is one solution to model II-A which corresponds closely to that of model II; however, axial heat conduction is sufficient to sustain an additional solution to model II-A which predicts light off. Under these conditions, model I-A also predicts two solutions, but, as usual, one of these is the unrealistic profile at the converter inlet. Also, if the Nusselt and Sherwood numbers in model I-A are reduced to 3.5, then model I-A predicts only a single solution, similar to the upper one in Figure 8. The results justify the entries in Table 3 under steady state 1c.

The calculations in Figure 8 are performed by using the kinetic expression *P2* in Table 1. Under similar conditions, multiple solutions could also be obtained by using expression *P1* in Table 1; however, from the difference between the solution to models II and II-A in Figure 5, the upper solution to model II-A would be much nearer the converter outlet. Kinetic expression *P2* can cause a much larger discrepancy between models II and II-A than that found in Figure 5 with *P1* kinetics. Other calculations suggest that if the solid diffusivity were changed to $D^f_{CO}/D^s_{CO} = 20$, then for the case in Figure 8 the upper solution to model II-A would lie much nearer to the converter inlet than for the case illustrated. The apparent reaction rate plays a large role in determining the effect of axial conduction in the wall. Figure 8 clearly shows the type of discrepancies encountered when model I-A is used and when the transverse diffusion and conduction in the fluid are neglected.

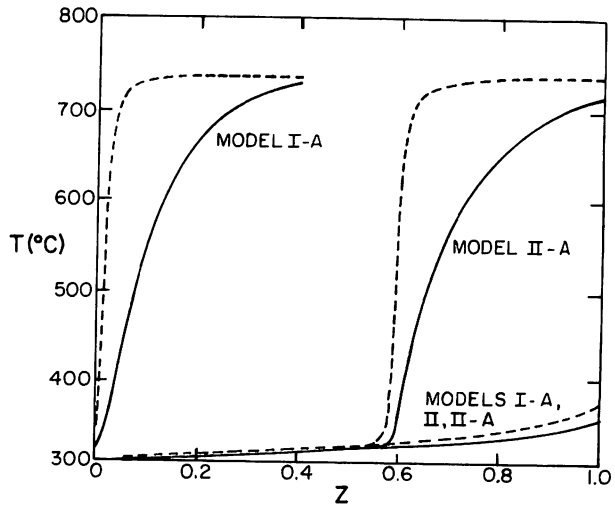

Fig. 8. Steady state model predictions for square geometry. Inlet T = 315°C, y_{CO} = 4%, $\hat{G}$ = 0.0151 m³/s, D^f_{CO}/D^s_{CO} = 70, ζ = 0.0254 mm. - - - - - Solid temperature, ——— Fluid average temperature. *P2* kinetics, model I-A: $Nu = Sh = 4.0$.

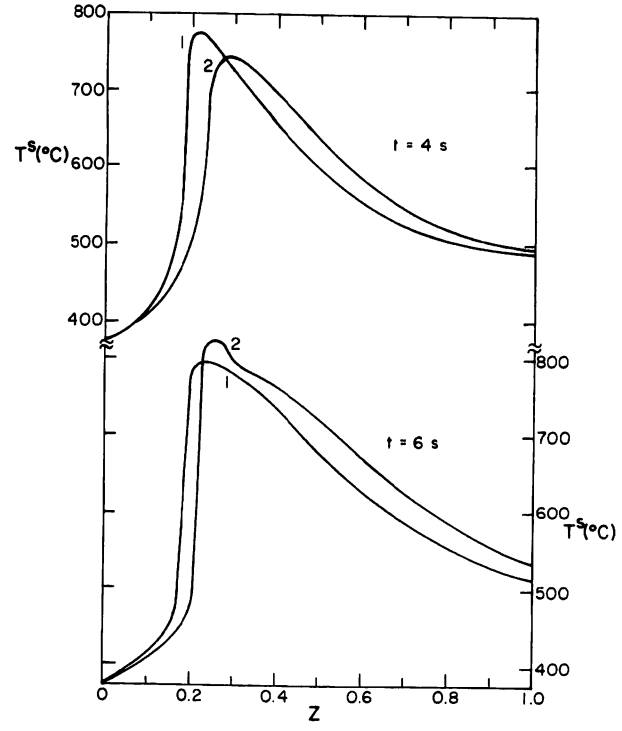

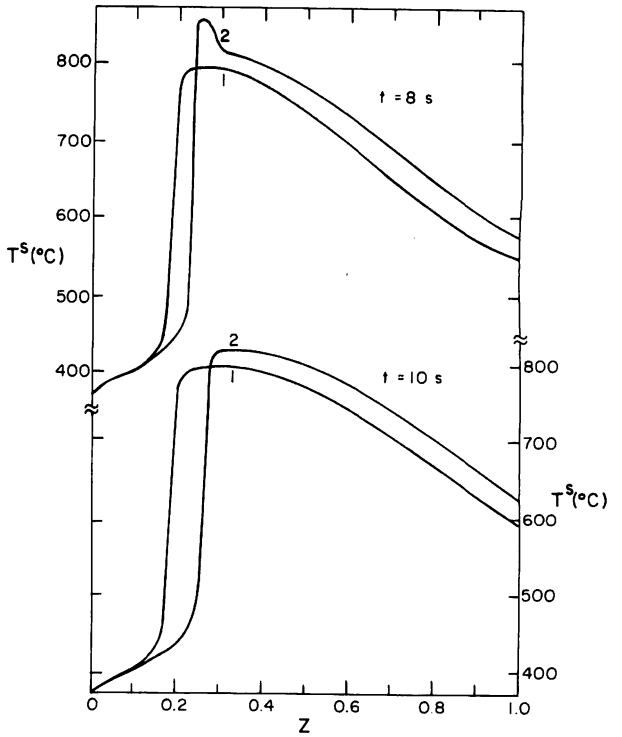

Fig. 9. Solid temperature during deceleration. 1—Model II-A for circle, 2—Model II for circle. *P1* kinetics. $t < 0$: $\hat{G}$ = 0.0377 m³/s, $y^f_0 = 0.01$, T_0 = 371°C; $t \geq 0$: $\hat{G}$ = 0.0134 m³/s, $y^f_0 = 0.04$, T_0 = 371°C.

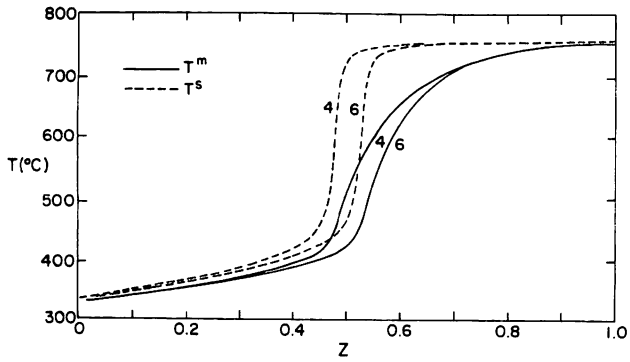

Fig. 10. Steady state model predictions for circle (6) and square (4). Inlet conditions as in Figure 5. ---- Solid temperature, ——— Fluid average temperature. P1 kinetics, model II-A.

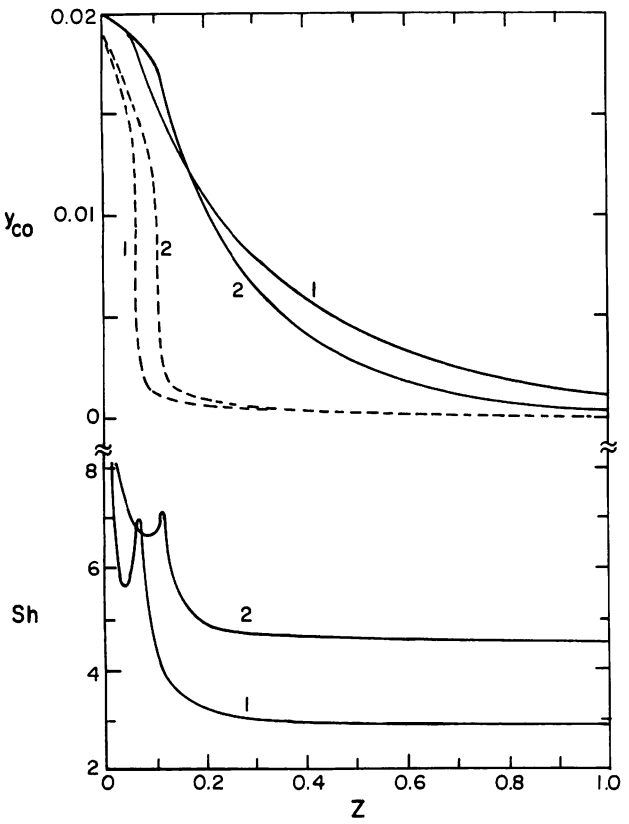

Fig. 11. Emission breakthrough for trapezoid (1) and rectangle (2): ----- y_{CO}^s, ——— y_{CO}^m. Inlet T = 427°C, y_{CO} = 2%, $\hat{G}$ = 0.0377 m³/s. P1 kinetics, model II-A.

For situations which exhibit a multiplicity of steady states, such as model I in Figure 5 and models I-A and II-A in Figure 8, the steady state eventually reached, with constant inlet conditions assumed, depends on the initial conditions of the monolith. If it is initially cold, the lower steady state will be realized, but if it is initially hot, the upper steady state will be realized. In these situations model I-A would not yield realistic results because light off occurs upstream of that predicted by model II-A in Figure 8 and is considerably upstream of the lowest steady state of model II-A in Figure 8. Indeed, model I-A may predict the reaction lights off, as in Figure 8, whereas in fact it does not.

Consider a transient example in which the inlet conditions change drastically, corresponding roughly to an automobile decelerating from a highway cruising speed.

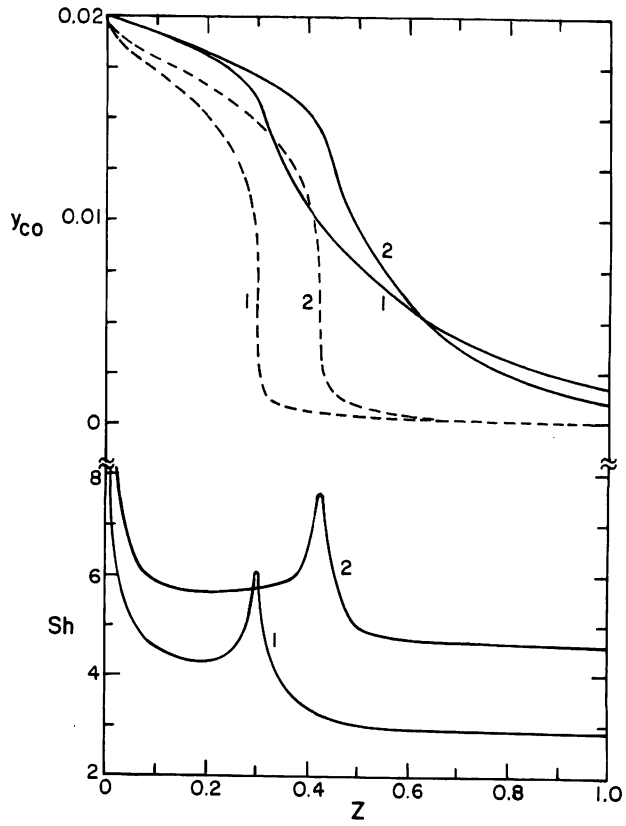

Fig. 12. Emission breakthrough for trapezoid (1) and rectangle (2): ----- y^sco, ——— y^mco, Inlet T = 371°C, y_{CO} = 2%, $\hat{G}$ = 0.0377 m³/s, P1 kinetics, model II-A.

The results predicted by models II and II-A are shown in Figure 9. As in the steady state, model II-A predicts a reaction zone which is closer to the inlet than predicted by model II. After 8 s, model II predicts a peak solid temperature which is 56°C above the adiabatic temperature. No such peak is predicted by model II-A, possibly because the effect of axial conduction tends to smooth out the peak as soon as it is formed. Model III-A (not shown) again agrees closely with model II-A for this case. Model I predicts a final steady state which is not the lowest one and is therefore erroneous. Model I-A would predict a final steady state similar to that in Figure 5, which is also erroneous.

In summary, the lumped parameter models (I and I-A) give incorrect results when they predict multiple steady states. Model II, with a distributed parameter fluid model used and with axial conduction neglected, gives reasonable predictions of the outlet conditions except in the region for which the addition of axial conduction (Model II-A) leads to another steady state. Model II does not usually give accurate predictions of the internal profiles in the converter. Model III-A, including peripheral conduction and diffusion, gives predictions similar to those of model II-A. Thus, the different phenomena can be rated in importance by transverse diffusion and conduction in fluid >> axial conduction in wall >> peripheral variations on the wall.

COMPARISON OF VARIOUS CELL SHAPES

A number of previous papers deal with the effects of the monolith cell shape on converter performance (Hegedus, 1973; Johnson and Chang, 1974; Heck et al 1974). These papers all deal solely with the limiting case of infinite reaction rate. In this case, the relative perform-

ance of different cell geometries can be determined by comparing the values of the asymptotic Sherwood numbers. Those with larger asymptotic Sherwood numbers give better performance. It is of interest to know how the cell shape affects converter performance for conditions less severe than this limiting one. Model calculations have been made for the cell shapes shown in Figure 2, and the effect of cell shape is compared on the basis established by Table 2.

The case in Figure 5 has also been calculated for circular geometry. In Figure 10, the results for circular and square geometry predicted by model II-A are compared. Owing to the poorer heat transfer in the square geometry, more heat accumulates at the wall, which increases the reaction rate and causes the reaction to light off nearer the inlet than in the circular duct. Thus, better transfer characteristics shift the reaction zone downstream; however, the degree of the shift is not substantial.

For the cases illustrated in Figures 5 and 10, all models and geometries predict essentially complete conversion. The effect of geometry will be most pronounced under conditions when complete conversion does not result.

Morgan et al. (1973) have discussed a phenomenon called emission breakthrough. Even though the converter is fully warmed up, some carbon monoxide can pass through unreacted. This phenomenon can occur when there is insufficient oxygen for complete conversion or owing to mass transfer limitations at high flow rates. When breakthrough occurs at high flow rates, the problem is most significant, since automobile emission standards are based on the weight of emissions. Examples of this type of situation are illustrated for model II-A in Figures 11 and 12. The calculations are performed for circular, square, rectangular, and trapezoidal cells, although only the results for the rectangle and trapezoid are illustrated. The results for the square and circle lie between those shown. The trapezoid cell with these aspect ratios is very similar to the corrugated monoliths currently in use and presumably will adequately predict the behavior of these monoliths.

The emission breakthrough, defined as the ratio of outlet to inlet carbon monoxide concentration, is shown in Table 4. In each case, the relative performance of each cell varies according to its asymptotic Sherwood number. Those with larger asymptotic Sherwood numbers have less breakthrough.

For the case with an inlet temperature of 427°C, the breakthrough with the trapezoidal cell is almost four times that for the rectangular cell, while for the 371°C inlet temperature case the ratio is less than two. The reasons for this result can be found by comparing Figures 11 and 12. In both cases the reaction zone for the trapezoid is nearer the inlet than that for the rectangle, but for the 371°C case the reaction zones are more widely separated than for the 427°C case. The reaction lights off earlier for the trapezoid, since the poor heat transfer allows the solid to reach a higher temperature which enhances the reaction. At the lower inlet temperature the reaction zones are more widely spaced because the reaction must proceed further before it will light off. Downstream from the reaction zone the good mass transfer characteristics of the rectangle is an asset, and the mixing cup mole fraction approaches zero in a much shorter length than with the trapezoid.

From the above discussion, it is apparent that a trade off exists in the performance of the various cell geometries. Converters with poor transferring geometries light off earlier than those with good transfer characteristics, and early light off enhances conversion. For those with good transfer characteristics, however, the mixing cup mole fraction approaches zero more quickly after the reaction zone. For the cases in Figures 11 and 12, the mixing cup mole fraction curves cross for all of the geometries, and good transfer characteristics prove to be advantageous. Under some conditions, when the breakthrough is greater than in these cases, for example, at higher flow rate or lower inlet temperature, the relative performance of the cell geometries will reverse and the mixing cup mole fraction curves will not cross. The emission breakthrough can be reduced by increasing the converter volume, and for a properly sized converter a cell geometry with good transfer characteristics is preferable for the basis of comparison used here. If the calculations were compared on a basis with constant pressure drop and superficial surface area, then the results would be more favorable to the trapezoid and rectangle.

The case in Figure 12 has been calculated by using the other models as well. Models II-A and III-A again agree closely, and in this case model II also gives good

Table 4. Predicted Emission Breakthrough

Model	Geometry	Breakthrough $y^m_{CO}\|_{z=1}/y^i_{CO,0}$	Sh_z
For Figure 11			
II-A	Rectangle	0.01396	4.44
II-A	Circle	0.02764	3.66
II-A	Square	0.04695	2.98
II-A	Trapezoid	0.05060	2.88
For Figure 12			
II-A	Rectangle	0.04906	4.44
II-A	Circle	0.06587	3.66
II-A	Square	0.08590	2.98
II-A	Trapezoid	0.08992	2.88
II	Square	0.08793	2.98
III-A	Square	0.08406	2.98
I-A	—	0.02017	4.00
I	—	0.01921-0.03981	4.44

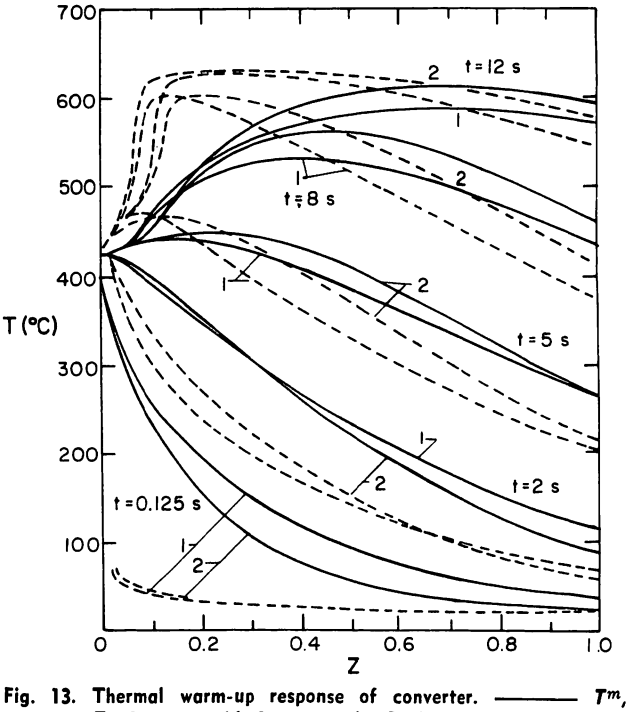

Fig. 13. Thermal warm-up response of converter. ——— T^m, - - - - - T^s, 1—trapezoid, 2—rectangle. P1 kinetics, model II-A.

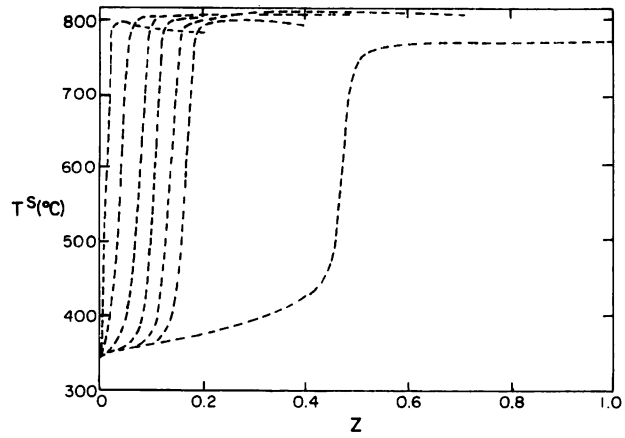

Fig. 14. Thermal cooling response of square cell monolith. Model II-A; curves from left to right are for t = 1, 5, 10, 15, 20, 25 s and steady state. P1 kinetics. For $t < 0$ T^s = 773°C; for $t \geq 0$ inlet conditions as in Figure 5.

agreement. The high flow rate used in this calculation reduces the effect of axial conduction. Model I again predicts an infinite number of steady states, and model I-A predicts a single unrealistic steady state with light off at the converter inlet.

The converter cell geometry affects not only emission breakthrough but could also affect the warm-up response of the converter. Converter warm-up is particularly important, since federal emission standards are based on a driving cycle which is initiated by a cold start. The converter warm-up response is illustrated in Figure 13 for rectangular and trapezoidal geometry. This transient has an initial solid temperature of 21°C, and at time zero the inlet conditions are changed to those in Figure 11.

The thermal response of the converter is quite fast for this ideal step change in conditions. With both geometries, the converter is nearly at steady state after only 12 s. The fast response in this case is due in part to the high flow rate; the response of the outlet mole fraction is even faster than the thermal response, and the outlet mole fraction reaches the steady state value in about 6 s in each case. Although the rectangular cell case warms up faster than the trapezoidal cell case, the effect is not large. The transfer characteristics of the different shaped ducts do not appear to have a substantial effect on the transient converter response.

Figure 13 also illustrates that the converter warms up most quickly at the inlet. This result is important. Model II, or any other model which neglects the mass transient and axial conduction and diffusion effects, predicts that the conditions at any point in the converter are not effected by the phenomena occurring downstream. Therefore, model II predicts that if the converter volume is increased to eliminate emission breakthrough, the outlet mole fraction will never be greater than in a smaller converter. The response of the outlet temperature will be slower, but not the outlet mole fraction. Although this reasoning is not strictly applicable to models II-A and III-A, it would presumably be approximately true, since the mass transient and axial conduction and diffusion effects are not usually large. There will generally be no penalty during transients in having a larger converter.

CONVERTER OVERTEMPERATURE

An important problem associated with both monolith and packed-bed converters is that under unusual conditions the substrate can melt, causing converter failure (Morgan et al., 1973). The exact nature of the inlet conditions which cause this problem are not known; however, it is reported to occur during sustained operation at high engine power and during descent down long hills, since high reactant concentrations result (National Academy of Sciences Report, 1972). Temperatures of approximately 1 370°C are required for melting to occur.

The most obvious explanation for this problem is that the inlet concentrations of carbon monoxide and hydrocarbons reach values large enough to result in an adiabatic temperature in excess of 1 370°C. For example, if the inlet temperature is 500°C and the inlet gas has a composition of 5% carbon monoxide, 1.7% hydrogen, and 1% propylene, the adiabatic temperature would be 1 400°C.

The adiabatic temperature is the maximum temperature that the outlet fluid can reach. The question should be, can the solid temperature ever exceed this value? The answer is yes, and two situations which can cause excess temperatures are discussed below.

For transients in which the front part of the converter cools, the solid temperature can exceed the adiabatic value. An example of this phenomenon is shown in Figure 14. For this case, the initial solid temperature is 773°C, and at time zero the inlet conditions are set at those for the case in Figure 5. The adiabatic temperature for the final state is also 773°C. During the transient, the solid temperature reaches a value 36°C in excess of the adiabatic temperature. Of course, these conditions are not extreme enough to cause melting, but the calculation does illustrate that temperatures in excess of the adiabatic value are possible. Other calculations suggest that the more extreme the conditions of temperature and composition the greater the overtemperature is likely to be. We note in Figure 9 that the inclusion of axial conduction (model II-A compared with model II) tends to reduce the peak overtemperature.

Overtemperature can also occur if the diffusivities of some species are large. Fast diffusing species can diffuse to the wall and react faster than the heat generated can be conducted away, causing temperatures in excess of the adiabatic value. In order for this phenomenon to occur, the Schmidt number for at least one reactant must be less than the Prandtl number. Hydrogen is the only specie present in exhaust gas (to any appreciable extent) which meets this criterion. Calculations and experiments demonstrating this phenomenon were reported by Hegedus (1974). However, Hegedus considered only the mass transfer limited situation with model I; that is, $y^s_{CO} \equiv 0$.

In Figure 15 a steady state calculation is illustrated in which hydrogen is modeled separately from carbon monoxide. In this case, the following data are assumed:

$$r_{H_2} = r_{CO}\frac{y_{H_2}}{y_{CO}}$$

$$H_{CO} = 256\,000 \text{ kJ/kg mole}$$

$$H_{H_2} = 244\,000 \text{ kJ/kg mole}$$

$$Sc_{H_2} = 0.15;\ y^f_{H_2,0} = 0.0133$$

The carbon monoxide kinetics and all other parameters are the same as those for the case illustrated in Figure 5; that is, this case reduces to the case in Figure 5 when the Schmidt number for hydrogen is changed to 0.7. The resulting solid temperature profiles predicted by models II and II-A are shown in Figure 15. For this case, the adiabatic temperature is again 773°C.

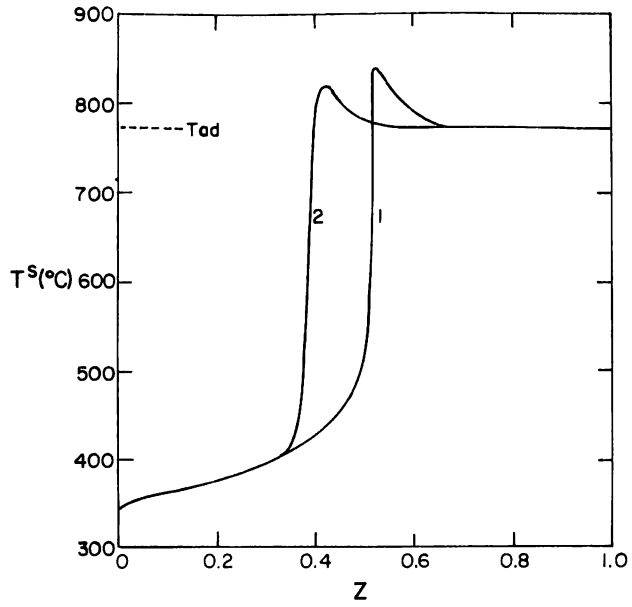

Fig. 15. Steady state solid temperature profile when hydrogen is modeled separately from carbon monoxide. Inlet conditions as in Figure 5. 1—Model II, 2—Model II-A, Pl kinetics, square cell.

Temperatures in excess of this value by 44° and 67°C are predicted by models II-A and II, respectively. Model II again predicts internal profiles different from the more accurate model II-A. Interestingly, the 44°C overtemperature results when the contribution of hydrogen to the total adiabatic temperature rise is only 104°C. The calculation illustrates that overtemperature can also occur owing to the presence of hydrogen in the exhaust gas. Presumably, in transients the overtemperature can be even larger.

ACKNOWLEDGMENT

Acknowledgment is made to the donors of the Petroleum Research Fund, administered by the American Chemical Society, for support of this research under Grant PRF No. 7698-AC7. We also acknowledge the suggestion of Prof. J. Wei to perform the calculations modeling hydrogen separate from carbon monoxide.

NOTATION

A_c = frontal area of monolith (m^2)
D = diffusivity
$\hat{G}$ = volumetric flow rate at standard conditions (m^3/s)
k_l = rate constant
L = length of monolith (m)
Nu = Nusselt number
r = rate of reaction, kg mole/sm^3
r_h = hydraulic radius, mm
Sh = Sherwood number
T = temperature (°K)
y = mole fraction
z = dimensionless length of monolith
ϵ = void fraction
ϵ_s = porous layer void fraction
ζ = thickness of porous layer (mm)

Superscripts

f = fluid
m = mixing cup average
s = solid

LITERATURE CITED

Eigenberger, G., "On the Dynamic Behavior of the Catalytic Fixed-Bed Reactor in the Region of Multiple Steady States I. The Influence of Heat Conduction in Two Phase Models," *Chem. Eng. Sci.*, **27**, 1909 (1972).

Finlayson, B. A., "Orthogonal Collocation in Chemical Reaction Engineering," *Cat. Rev.—Sci. Eng.*, **10**, 69 (1974).

Harned, J. L., "Analytical Evaluation of a Catalytic Converter System," *Soc. Auto Eng.*, paper 720520 (1972).

Heck, R. H., J. Wei, and J. R. Katzer, "The Transient Response of a Monolithic Catalyst Support," *Chem. Reaction Eng.-II, Adv. Chem. Ser.* **133**, 34 (1974).

Hegedus, L. L., "Effects of Channel Geometry on the Performance of Catalytic Monoliths," pp. 487-503 in Preprints of the Div. Petroleum Chem., 166th ACS meeting, Chicago, Ill. (Aug. 26-31, 1973).

———, "Temperature Excursions in Catalytic Monoliths," *Gen. Motors ret. GMR-1712, PCP-30* (1974).

Hlavácek, V., and J. Votruba, "Experimental Study of Multiple Steady States in Adiabatic Catalytic Systems," *Chem. Reaction Engng.-II, Adv. Chem. Ser.*, 133, 545 (1974).

Johnson, W. C., and J. C. Chang, "Analytical Investigation of the Performance of Catalytic Monoliths of Varying Channel Geometries Based on Mass Transfer Controlling Conditions," Soc. Auto. Eng., paper 740196 (1974).

Kuo, J. C. W., private communication (1973).

Kuo, J. C. W., H. G. Lassen, and C. R. Morgan, "Mathematical Modeling of CO and HC Catalytic Converter Systems," Soc. Auto. Eng., paper 710289 (1971).

Langmuir, I., "The Mechanism of the Catalytic Action of Platinum in the Reactions $2CO + O_2 = 2CO_2$ and $2H_2 + O_2 = 2H_2O$," *Trans. Faraday Soc.*, **17**, 621 (1922).

Liu, S. L., and N. R. Amundson, "Stability of Adiabatic Packed Bed Reactors. An Elementary Treatment," *Ind. Eng. Chem. Fundamentals*, **1**, 200 (1962).

Morgan, C. R., D. W. Carlson, and S. E. Voltz, "Thermal Responses and Emission Breakthrough of Platinum Monolithic Catalytic Converters," Soc. Auto. Eng., paper 730569 (1973).

National Academy of Sciences, semiannual report by the Committee on Motor Vehicle Emissions to the Environmental Protection Agency (Jan., 1972).

Schlatter, J. C., R. L. Klimisch, and K. C. Taylor, "Exhaust Catalysts: Appropriate Conditions for Comparing Platinum and Base Metal," *Science*, **179**, 798 (1973).

Sklyarov, A. V., I. I. Tret'yakov, B. R. Shub, and S. Z. Roginskii, "Oxidation of Carbon Monoxide by Oxygen on Platinum Purified in Ultra-high Vacuum," *Dokl. Phys. Chem.*, **189**, 829 (1969).

Voltz, S. E., C. R. Morgan, D. Liederman, and S. M. Jacob, "Kinetic Study of Carbon Monoxide and Propylene Oxidation on Platinum Catalysts," *Ind. Eng. Chem. Prod. Res. Develop.*, **12**, 294 (1973).

Votruba, J., J. Sinkole, V. Hlavácek, and J. Skrivánek, "Heat and Mass Transfer in Monolithic Honeycomb Catalysts-I," *Chem. Eng. Sci.*, **30**, 117 (1975).

Wei, J., "Catalysis for Motor Vehicle Emissions," *Advan. Catalysis*, **24**, 57 (1975).

Young, L. C., and B. A. Finlayson, "Mathematical Modeling of the Monolith Converter," *Chem.-Reaction Eng.-II, Adv. Chem. Ser.*, **133**, 629 (1974).

Young, L. C., "The Application of Orthogonal Collocation to Laminar Flow Heat and Mass Transfer in Monolith Converters," Ph.D. thesis, Univ. Wash., Seattle (1974).

Manuscript received August 26, 1976; revision received December 1, and accepted December 4, 1975.